Experimental Study of Friction Welding of Incompatible Materials: Interlayer Metals and Parameter Modifications

Sayyad Shaik [1], Dr. P. Ravinder Reddy[2], Dr. P. Laxminarayana[3]

[1] Research Scholar, Osmania University, Hyderabad, Telangana, India

[2] Professor & HOD, Department of Mechanical Engineering, CBIT, Hyderabad, Telangana, India

[3] Professor & Registrar, UCE, Osmania University, Hyderabad, Telangana, India

Email: [1] sayyad4915@gmail.com

Abstract

The aim of this research is to investigate the development and evaluation of solid-state bonds between dissimilar materials, particularly Copper and Brass, by incorporating naval brass as an interlayer and change in friction parameters using the drive friction welding technique. This innovative approach utilizes the heat generated through friction between two surfaces, resulting in plastic deformation. During the experimental phase, a comprehensive exploration of various welding process parameters was carried out. Subsequently, the outcomes underwent a thorough analysis, which included tensile testing, Vickers micro-hardness testing, and conducting analysis through SEM-EDX (energy dispersive X-ray).. These analyses played a pivotal role in identifying the phases formed during the welding process.

Keywords: Friction Welding (FW), Dissimilar Material, Welding of Copper, Brass and Naval Brass.

1. Introduction

Friction welding is widely acknowledged as a manufacturing process utilized across various industries, including switchgear, oil gas and automotive sectors, to join both similar and dissimilar materials. While it offers great versatility, there are occasional instances where the resulting joints do not meet desired quality standards. Interestingly, there are cases where this technique demonstrates exceptional strength, surpassing even the weaker sections of the two base metals being joined. The central objective of the research presented here is to evaluate the potential of a modified friction welding process for bonding incompatible materials. This paper explores the outcomes achieved through this method, which has proven effective in addressing situations where brittle welds or complete welding failure were previously encountered.

2. Literature Survey

Friction welding exemplifies a prominent instance of a metal joining process involving solid-state techniques. Within this technique, mechanical energy is skillfully transformed into thermal energy specifically at the workpieces' interface, resulting in the generation of heat. This phenomenon occurs as the workpieces rotate under substantial pressure. The versatility of friction welding becomes evident in its ability to effectively bond various ferrous and non-

ferrous alloys, regardless of their cross-sectional shape, be it circular or non-circular. These materials often possess distinct thermal and mechanical properties, highlighting the adaptability of friction welding.

Categorized within the domain of solid-state welding methods, friction welding enables the establishment of a metallurgical bond at temperatures lower than the melting point of the constituent base metals. The American Welding Society (AWS) has acknowledged friction welding as a solid-state welding technique in which the welding process takes place as the workpieces rotate or move in respect to one another. This action causes the material at the contact surfaces to deform plastically, producing heat. Even though it is referred to be a solid-state process, the interface occasionally has a molten film. However, the final weld often does not show obvious signs of being in a molten state because to the intensive hot working that occurs in the latter phases of the process. As opposed to many other welding techniques, friction welding has minimum material needs since it doesn't require filler metal, flux, or shielding gases. With its inherent simplicity, friction welding becomes even more appealing in various industrial applications, as illustrated in Figure 1 showcasing the visual depiction of its basic steps..

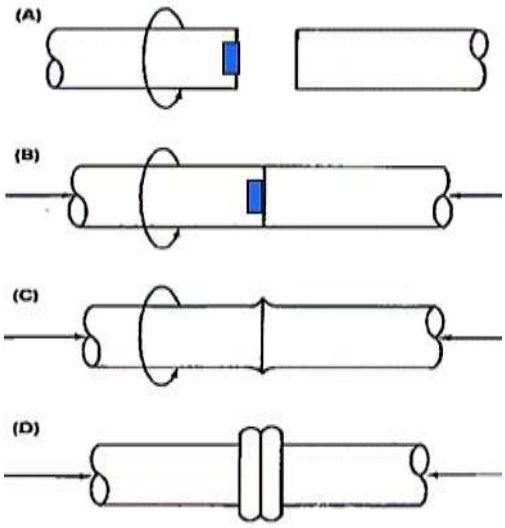

Figure 1. The basic steps in friction welding

F. Sassani et al. [1], offers a comprehensive overview of the most commonly joined dissimilar materials within the industrial context. It sheds light on numerous challenges associated with welding dissimilar materials, including variations in melting points, differences in cast structures at the interface, the presence of inclusions, and issues related to micro-segregation. Furthermore, the study highlights an intriguing aspect of friction welding: its ability to weld certain similar materials that are traditionally considered non-weldable using conventional welding techniques. Surprisingly, friction welding has proven effective in these scenarios. Notably, in the majority of friction welding applications involving both similar and dissimilar materials, the resulting strength exceeds that of the weaker material being joined. This remarkable attribute has elevated friction welding to the status of the preferred method whenever the size and geometry of the workpiece permit its application.

Kimura et al. [2] conducted a meticulous examination of the influence of friction welding parameters on various aspects of the joining process between pure Aluminum (CP-Al) and austenitic stainless steel (AISI304). The objective was to assess the impact of these conditions on joining phenomena, tensile strength, and bend ductility of the friction-welded joints. Remarkably, the research revealed the possibility of achieving high joint efficiency, characterized by a fracture occurring on the CP-Al side without any cracks at the weld interface and the absence of an intermetallic compound (IMC) interlayer at the weld interface. To achieve such successful joints, the study recommended specific friction welding conditions. Firstly, the joint should be forged with substantial pressure of 150 MPa. Additionally, it was crucial to pinpoint the opportune friction time, during which the temperature at the weld interface reached approximately 573 K or higher. These prescribed friction welding conditions were found to be instrumental in producing high-quality joints with both exceptional joint efficiency and remarkable bend ductility, up to an angle of 90 degrees.

Liang et al. [3], the focus was on joining a 5A33 aluminum alloy bar with an AZ31B magnesium alloy bar using continuous drive friction welding. During their investigation, they observed a noteworthy trend in the tensile strength of the joints. As the friction time increased, there was a corresponding increase in the tensile strength of the joints. On average, the highest tensile strength recorded was an impressive 101 MPa, which occurred at a friction time of 5 seconds. Interestingly, all the samples subjected to friction welding exhibited a unique failure pattern, as fractures consistently occurred at the friction interface during tensile testing. The visual appearance of these fractures displayed nearly flat surfaces, indicative of a brittle mode of failure in the as-welded Al/Mg joints investigated in this experiment. Notably, a distinctive reaction layer formed at the friction interface, comprising intermetallic compounds (IMCs) and a solid solution of Mg. The primary IMCs identified were Mg17Al12 and Al3Mg2, and their composition varied with the duration of the friction process. This reaction layer possessed significantly high micro-hardness, resulting in a dramatic increase in micro-hardness values at the interface compared to the base material of the Mg side. Moreover, the thickness of the hardened layer in the Mg side and the softened layer in the Al side grew progressively thicker with increasing friction time.

Pandia Rajan et al. [4] engaged in the friction welding of two dissimilar materials, specifically SA 213 tube and SA 387 tube plate. Their objective was to utilize an external tungsten carbide tool to both enhance and validate the mechanical and metallurgical properties of the resulting joints. The investigation involved two distinct types of materials. Type 1 represented tubes without holes, while Type 2 denoted tubes with holes positioned along their circumference. The research yielded some noteworthy findings. Optimal Joint Strength: It was observed that the optimal joint strength for the workpiece without a hole reached an impressive 2980 MPa, while the workpiece with a hole exhibited a slightly lower but still substantial joint strength of 2680 MPa. Vickers Hardness Test: The Vickers hardness test, employed to gauge the hardness of the welded zone, revealed significant differences between the two types of workpieces. In the workpiece without a hole, the Vickers hardness value was notably higher at 292 Hv, while in the workpiece with a hole, it measured at a

slightly lower 217Hv.These findings underscore the influence of the presence or absence of a hole on the mechanical and metallurgical properties of the welded joints, with the workpiece without a hole consistently displaying superior joint strength and hardness characteristics.

3. The Experimental Procedure

A. Dissimilar Materials Used

During the experiment, two different materials, namely Copper and Brass, were employed. Extensive chemical composition analyses were carried out using Optical Emission Spectroscopy (OES) at a metallurgical testing facility for both Copper and Brass. The outcomes of these chemical analyses are presented in the subsequent tables. Table 1 provides the chemical composition obtained from the analysis of copper, while Table 2 displays the chemical composition obtained from the analysis of Brass. Chemical composition obtained by chemical analysis of Naval Brass is given in Table 3.

Table 1. Chemical composition of copper

Elements	Symbol	Unit	Specified values	Observed values
Copper	C	%	99.94	99.91
Phosphorous	P	%	0.045Max	0.035

Table 2. Chemical composition of Brass

Elements	Symbol	Unit	Specified Values	Weight
Copper	C	%	60-65	63.5
Zinc	Zn	%	35-37	34.5

Table 3. Chemical composition of Naval Brass

Elements	Symbol	Unit	Specified Values
Copper	C	%	60-63
Tin	Sn	%	.8-1.1
Zinc	Zn	%	36-41

B. Specifications of machine

The specifications of the Friction welding machine are shown in Table 4 friction welded joint.

Figure 2. Experimental Friction welding machine setup

Table 4. Specifications of the Friction welding machine

F.W.M/c Type	FWT-5
Max weld area	800 mm2
Min weld area	70mm2
Max bar capacity (solid dia)	32mm
Min bar capacity (solid dia)	10mm
Max length of rotating component	220mm
Max length of non-rotating component	300mm
Max forge force	120KN
Spindle speed variable	1000-2000RPM
Spindle bore depth from collet face	200mm
Slide stroke	350mm
Total connected wattage	30KVA
Supply voltage	400V/50HZ
Spindle drive	15KW
Control voltage	24VDC

C. Geometry of the Samples with dimensions

The specimens were painstakingly created from the materials by carefully following the prescribed dimensions. The specimen sizes for copper and brass are as follows:

1. Copper Specimen:
    i. Length: 100mm
    ii. Outer Diameter: 12.7mm
2. Brass Specimen:
    iii. Length: 100mm
    iv. Outer Diameter: 12.7mm
3. Naval Brass Specimen:
    v. Thickness: (1,1.2,1.4,1.6,1.8 and 2.0) mm
    vi. Outer Diameter: 10mm

These precise dimensions were carefully followed in the machining of the specimens, ensuring that the variations in inner extruded parts for Copper and Brass, as well as the thickness changes in the Naval Brass specimen, were accurately achieved for the experimental setup. All the dimensions are depicted in Fig 3.

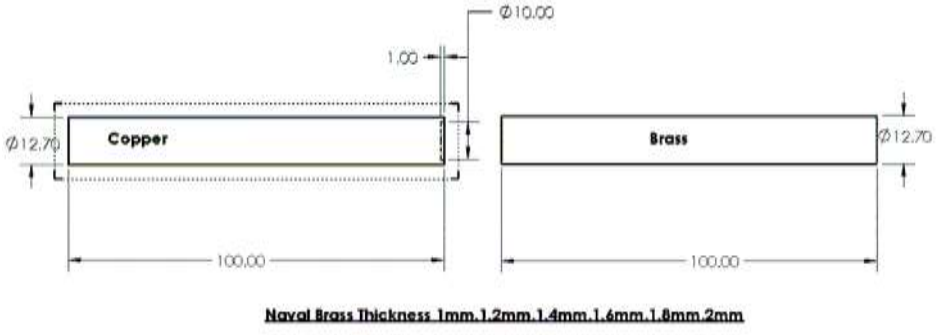

Figure 3. Geometry of specimen using Naval Brass as Interlayer

D. Experimental Parameters for Friction Welding

The main parameters used for the present work to perform the friction welding are: Pressure P1 (friction pressure) and time t1 (friction time)- heating phase; Pressure P2 (upset pressure) and time t2 (upset time)- forging phase; and rotation per minute (RPM).

The various parameters adapted/used for the present work is given in the table 5 and table 6.

Table 5: Using Naval Brass as Interlayer with friction welding parameters fixed.

Number of trails	Naval Brass Thickness (mm)	Friction Pressure (Mpa)	Friction Time (s)	Upset Pressure (MPA)	Upset Time(s)	Rotational Speed (RPM)
1	1	34.47	1.5	77.56	10	1120
2	1.2	34.47	1.5	77.56	10	1120
3	1.4	34.47	1.5	77.56	10	1120
4	1.6	34.47	1.5	77.56	10	1120
5	1.8	34.47	1.5	77.56	10	1120
6	2.0	34.47	1.5	77.56	10	1120

Table 6: No interlayer and Changing Friction speed

Number of trails	Friction Pressure (Mpa)	Friction Time (s)	Upset Pressure (MPA)	Upset Time(s)	Rotational Speed (RPM)
1	34.47	1.5	77.56	10	1120
2	34.47	1.5	77.56	10	1200
3	34.47	1.5	77.56	10	1300
4	34.47	1.5	77.56	10	1400
5	34.47	1.5	77.56	10	1500
6	34.47	1.5	77.56	10	1600
7	34.47	1.5	77.56	10	1700
8	34.47	1.5	77.56	10	1800
9	34.47	1.5	77.56	10	1900

4. RESULTS AND DISCUSSIONS

A. Tensile test

Following the completion of welding, tensile tests were conducted to assess the mechanical properties of the joints. These tests aimed to optimize and qualify the welding procedures and processes, in addition to evaluating parameter settings. The welded specimens were machined in accordance with ISO 15620 standards for friction welding, with their dimensions outlined in Table 5. Subsequently, they underwent tensile testing using a machine equipped with a load cell capacity of 120 KN at a room temperature of 25°C. Figure 4 provides a visual representation of the weld joint specimen prepared for the tensile test.

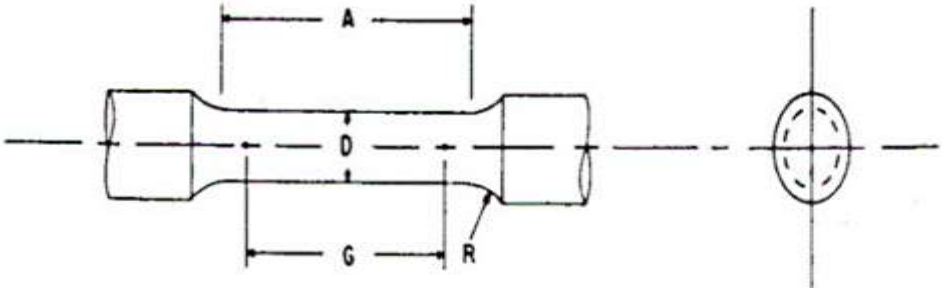

Figure 4. Weld joint specimen prepared for the tensile test

Table 5. For Test Specimens with Gauge Length Four times the Diameter

Specifications	Standard Specimen Dimensions(mm)
G-Gauge Length	36
D-Diameter	9
R-Radius of fillet, in	8
A-Length of reduced section,	45

In a previous study conducted by F. Sassani et al. [1], the effects of upset time, upset pressure, friction time, friction pressure, and friction speed of joints were examined in the welding of equal diameter parts. The strength of the joints was determined through tensile tests and compared to fully machined specimens. In this investigation, the addition of rotational speed was expected to bring about a change.

Table 6 provides the obtained tensile strength for the six corresponding trials. The tensile strength of the joints was estimated by dividing the ultimate load by the area of a 9 mm diameter specimen. It was found that the fracture occurred at the interface of the dissimilar metal weld joint. The strength of the weld joint was lower than the tensile strength of brass (338 MPa), but higher than that of copper (210 MPa).

The results obtained from the testing, which are shown graphically in Figure 5, indicate that as the thickness of the naval brass increases, the bonding of the joints also increases up to a certain extent. Consequently, the tensile strength of the joints also increases. However, the strength of the joints reaches a maximum and then begins to decrease as the naval brass thickness increases further. This is due to a decrease in mechanical locking or elemental bonding between the two dissimilar metals. It is evident that naval brass thickness directly affects the joint quality, while upset time and pressure also have an impact on the bonding of the metals in the weld. Additionally, it was found that the joint was slightly softened but still maintained its mechanical integrity

Table 6. Tensile strength values using Naval Brass Interlayer

Number of trails	Naval Brass Thickness (mm)	Friction Pressure (Mpa)	Friction Time (s)	Upset Pressure (MPA)	Upset Time (s)	Rotational Speed (RPM)	UTS (MPA)
1	1	34.47	1.5	77.56	10	1120	206
2	1.2	34.47	1.5	77.56	10	1120	211
3	1.4	34.47	1.5	77.56	10	1120	213

Number of trails	Naval Brass Thickness (mm)	Friction Pressure (Mpa)	Friction Time (s)	Upset Pressure (MPA)	Upset Time (s)	Rotational Speed (RPM)	UTS (MPA)
4	1.6	34.47	1.5	77.56	10	1120	162
5	1.8	34.47	1.5	77.56	10	1120	110
6	2.0	34.47	1.5	77.56	10	1120	72

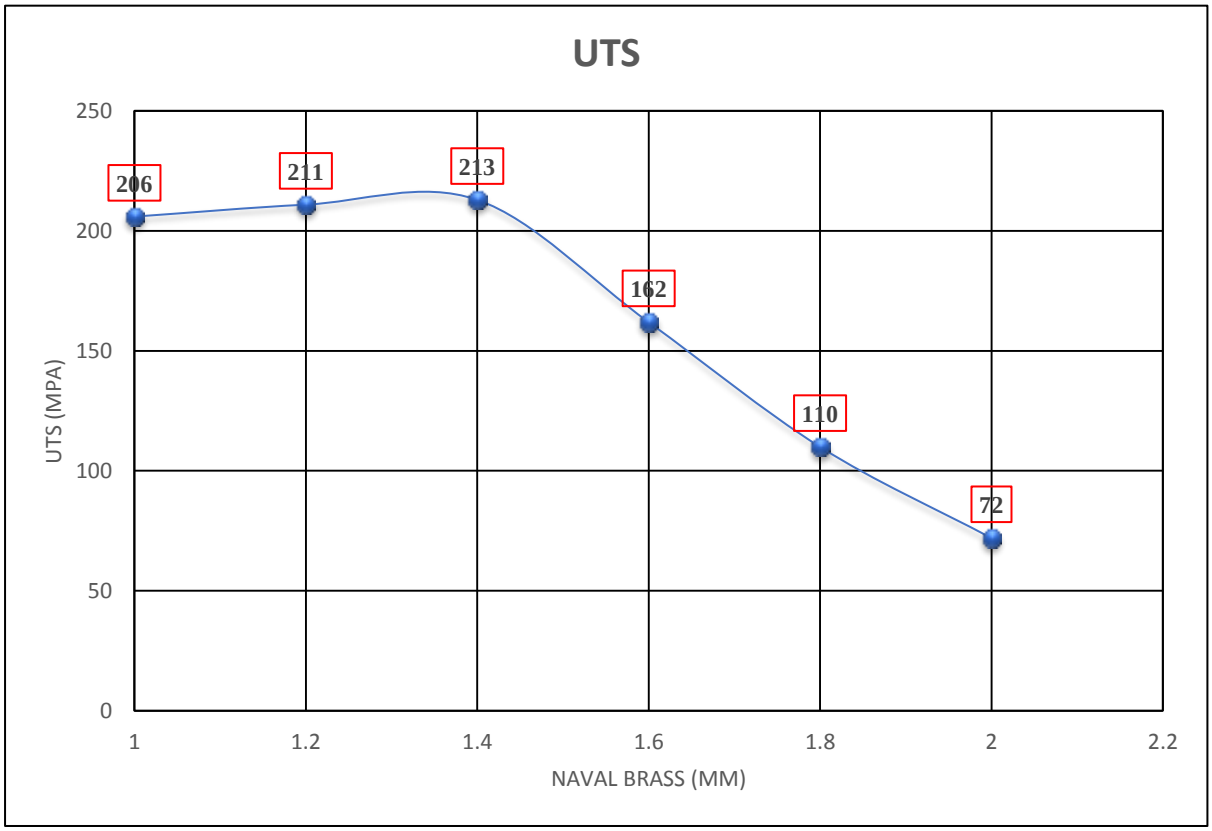

Figure 5. Friction Welding of Brass and Copper using Naval Brass Interlayer

Table 7 provides the obtained tensile strength for the nine corresponding trials. The tensile strength of the joints was estimated by dividing the ultimate load by the area of a 9 mm diameter specimen. It was found that the fracture occurred at the interface of the dissimilar metal weld joint. The strength of the weld joint was lower than the tensile strength of brass (338 MPa), but higher than that of copper (210 MPa).

The results obtained from the testing, which are shown graphically in Figure 6, indicate that as the rotational speed increases, the bonding of the joints also increases up to a certain extent. Consequently, the tensile strength of the joints also increases. However, the strength of the joints reaches a maximum and then begins to decrease as the rotational speed increases further. This is due to a decrease in mechanical locking or elemental bonding between the two dissimilar metals. It is evident that rotational speed directly affects the joint quality, while upset time and pressure also have an impact on the bonding of the metals in the weld. Additionally, it was found that the joint was slightly softened but still maintained its mechanical integrity.

Table 7. Tensile strength values with no Interlayer and change in friction speed

Number of trails	Friction Pressure (Mpa)	Friction Time (s)	Burn-off Length(mm)	Upset Pressure (MPA)	Upset Time (s)	Rotational Speed (RPM)	UTS (MPA)
1	34.47	1.5	3.5	77.56	10	1120	0
2	34.47	1.5	3.5	77.56	10	1200	0
3	34.47	1.5	3.5	77.56	10	1300	0
4	34.47	1.5	3.5	77.56	10	1400	0
5	34.47	1.5	3.5	77.56	10	1500	142.77
6	34.47	1.5	3.5	77.56	10	1600	156.34
7	34.47	1.5	3.5	77.56	10	1700	234.68
8	34.47	1.5	3.5	77.56	10	1800	254.46
9	34.47	1.5	3.5	77.56	10	1900	0

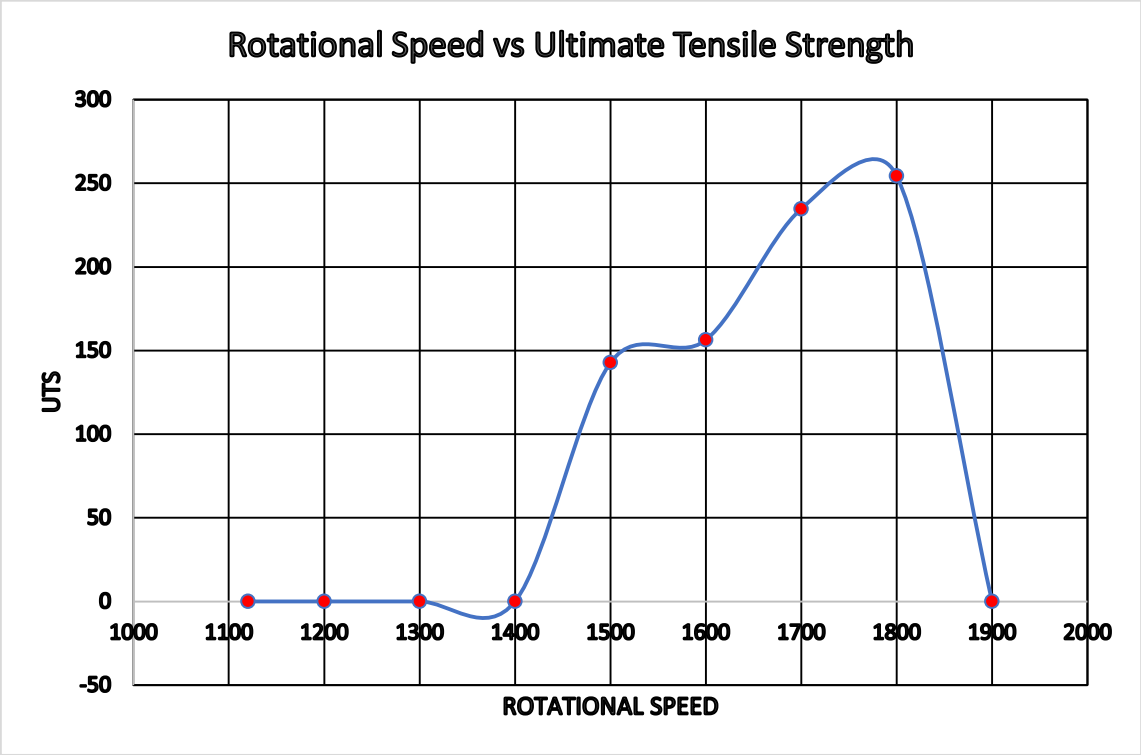

Figure 6. Friction Welding of Brass and Copper

B. Vickers Micro Hardness Test

The strength of the joints is correlated with the variation in hardness within the Heat-Affected Zone (HAZ). Hardness variations were determined using micro hardness testing under a HV10 load, employing a digital Vickers hardness testing machine. Micro hardness assessments were performed at the weld interface and in areas adjacent to both the Copper and Brass sides. Figure 7 illustrates the hardness variations across the horizontal distance from the center within the welding zone of the joints.

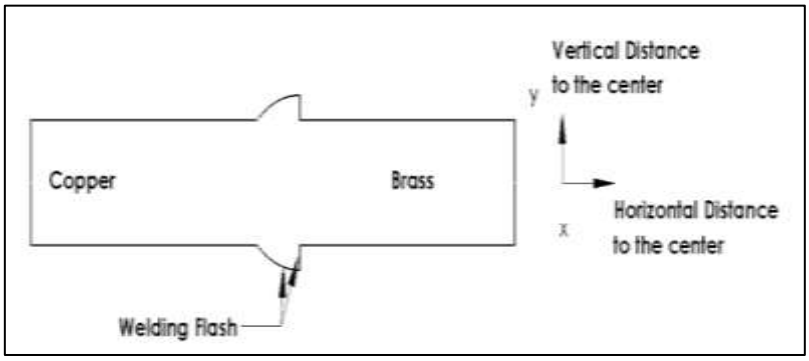

Figure 7. Hardness test orientation

Table 7 Vicker hardness results (Naval Brass Interlayer)

NO. Of Trials	Naval Brass Thickness (mm)	Friction Pressure (Mpa)	Friction Time (s)	Upset Pressure (MPA)	Upset Time (s)	Rotational Speed (RPM)	UTS (MPA)	Copper Hardness (HV10)	Middle Weld (HV10)	Brass (HV10)
1	1	34.47	1.5	77.56	10	1120	206	80	103	125
2	1.2	34.47	1.5	77.56	10	1120	211	79	105	134
3	1.4	34.47	1.5	77.56	10	1120	213	77	106	139
4	1.7	34.47	1.5	77.56	10	1120	162	78	102	131
5	1.9	34.47	1.5	77.56	10	1120	110	81	99.5	143
6	2.0	34.47	1.5	77.56	10	1120	72	78	98.5	145

Micro-hardness test results with respect to the horizontal distance from the center are shown in Table 7 Increase in hardness corresponds to the brass side. A heat affected zone (HAZ) with a small width was formed that resulted in softening of the naval brass alloy. As the naval brass used in the present study was a cold-drawn bar, it was already work-hardened before the friction welding process. The naval brass recovered and recrystallized as a result of forging heat and deformation, thus was slightly softened. As shown in Fig. 8, the hardness on the copper side of the joints decreases as it is advanced towards the end of the parts. On the other hand, hardness on the brass side of the joints increases significantly.

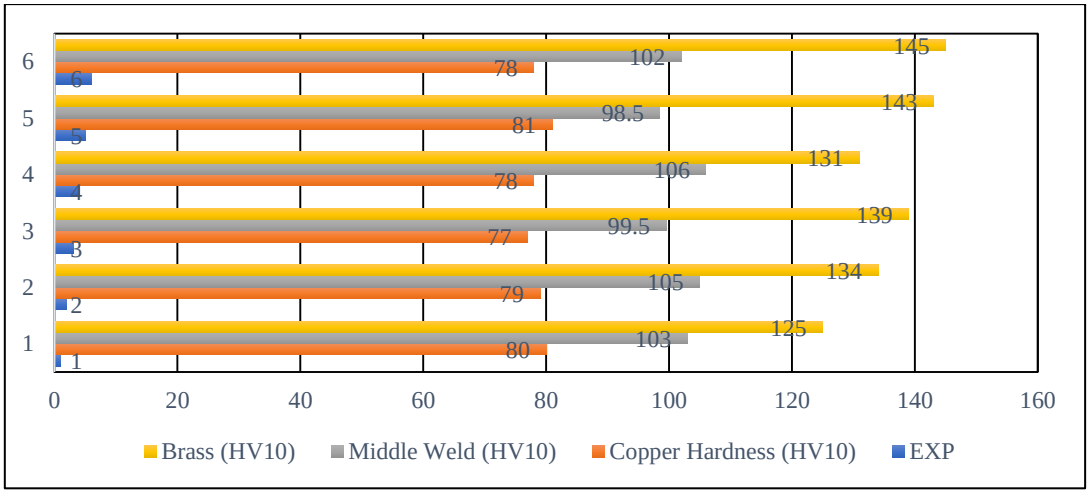

Figure 8. Hardness test results (HV-10) (Naval Brass Interlayer)

Micro-hardness test results with respect to the horizontal distance from the center are shown in Table 8 Increase in hardness corresponds to the brass side. A heat affected zone (HAZ) with a small width was formed that resulted in softening of the rotational speed. As shown in Fig. 9, the hardness on the copper side of the joints decreases as it is advanced towards the end of the parts. On the other hand, hardness on the brass side of the joints increases significantly.

Table 8. Vicker hardness results (No Interlayer)

NO. Of Trials	Friction Pressure (Mpa)	Friction Time (s)	Burn-off Length (mm)	Upset Pressure (MPA)	Upset Time (s)	Rotational Speed (RPM)	UTS (MPA)	Copper Hardness (HV10)	Middle Weld (HV10)	Brass (HV10
1	34.47	1.5	3.5	77.56	10	1120	0	82	0	131
2	34.47	1.5	3.5	77.56	10	1200	0	81	0	134
3	34.47	1.5	3.5	77.56	10	1300	0	80	0	135
4	34.47	1.5	3.5	77.56	10	1400	0	79	0	139
5	34.47	1.5	3.5	77.56	10	1500	142.77	78	55.74	142
6	34.47	1.5	3.5	77.56	10	1600	156.34	77	61.04	143
7	34.47	1.5	3.5	77.56	10	1700	234.68	76	91.63	149
8	34.47	1.5	3.5	77.56	10	1800	254.46	74	99.36	154
9	34.47	1.5	3.5	77.56	10	1900	0	78	0	145

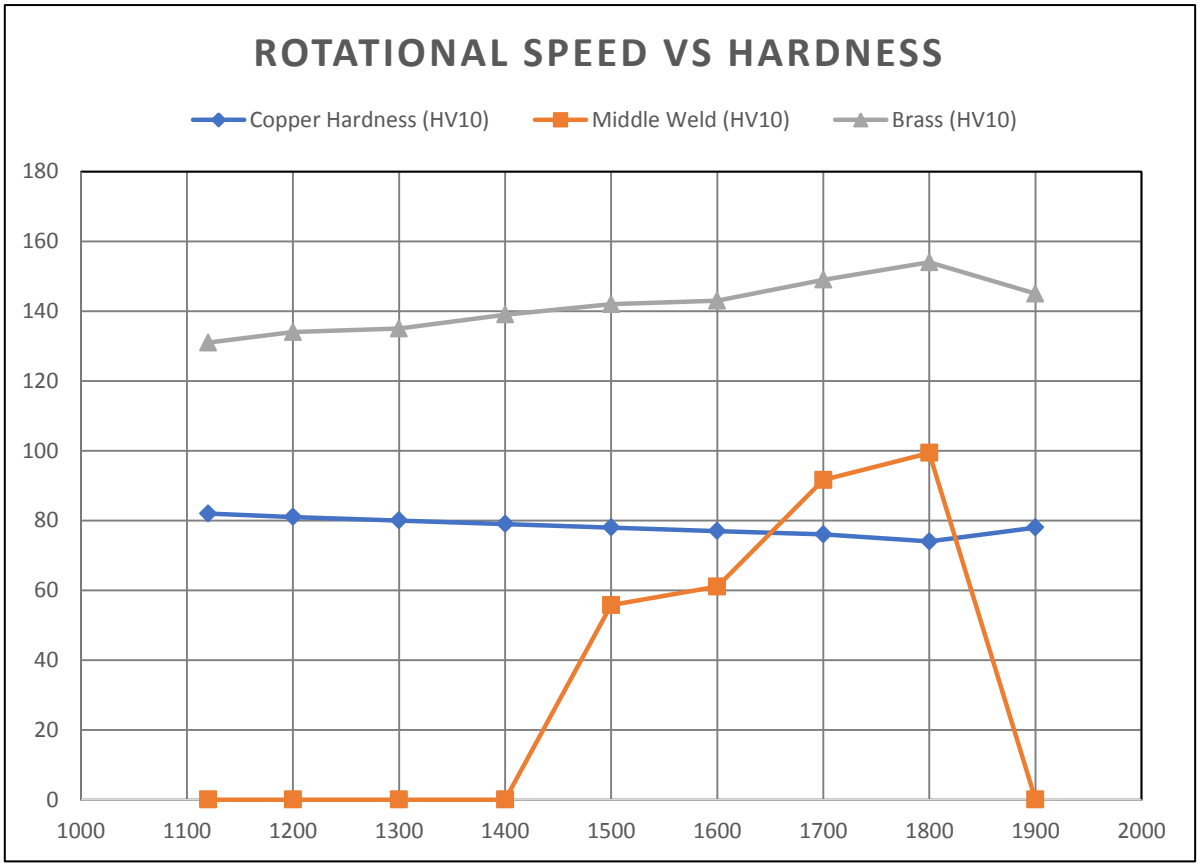

Figure 9. Hardness test results (HV-10) (No Interlayer)

C. Impact Test

The Charpy impact test, also known as the Charpy V-notch test, is a standardized assessment of a material's ability to absorb energy during fracture under high strain rates. This absorbed energy serves as a measure of the material's toughness. It is widely adopted in industry due to its ease of preparation and execution, as well as the rapid and cost-effective acquisition of results. However, a significant limitation lies in the comparative nature of the results. For the present study, the standard test specimens were prepared in accordance with ASTM E23, featuring a length of 55 mm and a square cross-section with sides measuring 10 mm. At the center of this length, a V-notch with a 45° angle, 2 mm depth, and a 0.25 mm radius of curvature at the base was created. The dimensions of the Charpy V-notch are illustrated in Figure 10 below.

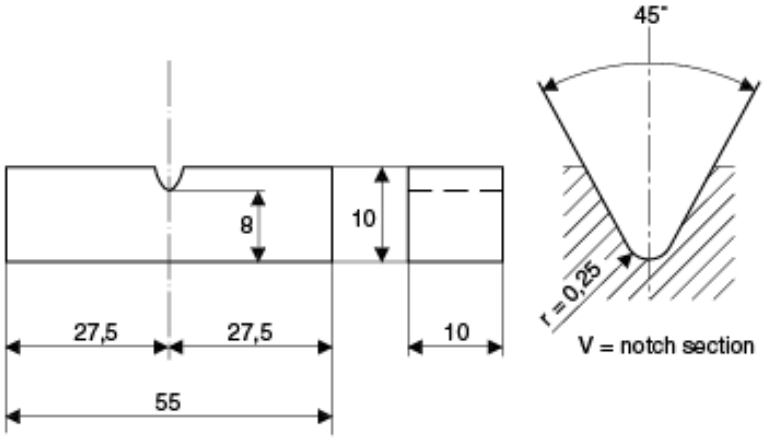

Figure 10. Charpy V-notch dimensions

The results found for six different Naval brass thickness were given in the table 9 and respective graph shown in fig 11, which gives us the clear view that the specimen weld joint of trial 2 and 3 had absorbed more energy 14.2 and 14.5 joules respectively compare to trial 1 and gradually decreased as Naval brass thickness increases, representing that it bears more toughness, since the resistance to applied load (hammer impact) at the weld joint interface is more because the quality of bonding between the two dissimilar metals was sound.

Table 9. Energy absorbed by the weld joints (Naval Brass Interlayer)

Number of trails	Naval Brass Thickness (mm)	Friction Pressure (Mpa)	Friction Time(s)	Upset Pressure (MPA)	Upset Time(s)	Rotational Speed (RPM)	UTS (MPA)	Joules Energy (J)
1	1	34.47	1.5	77.56	10	1120	206	13
2	1.2	34.47	1.5	77.56	10	1120	211	14.2
3	1.4	34.47	1.5	77.56	10	1120	213	14.5
4	1.7	34.47	1.5	77.56	10	1120	162	8
5	1.9	34.47	1.5	77.56	10	1120	110	1.2
6	2.0	34.47	1.5	77.56	10	1120	72	0

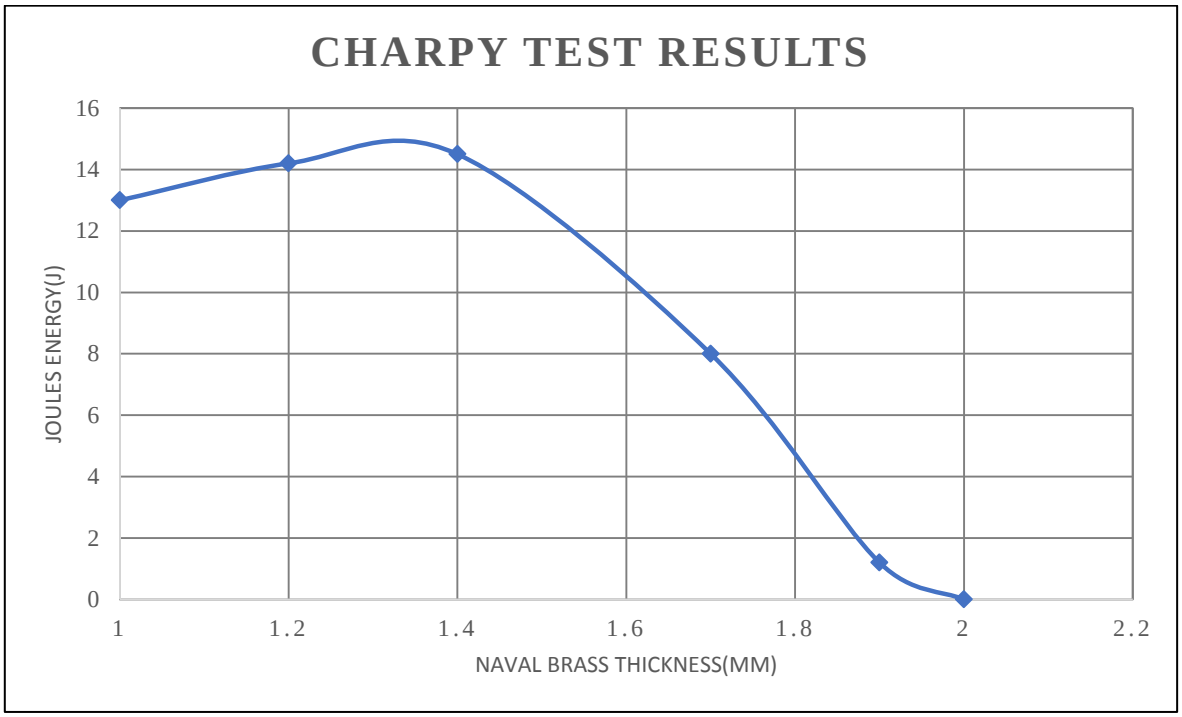

Figure 11. Joules Energy (Naval Brass Interlayer)

The results found for 9 different rotational speed were given in the table 10 and respective graph shown in fig 12, which gives us the clear view that the specimen weld joint of trial 7 and 8 had absorbed more energy 14.2 and 14.5 joules respectively compare to trial 1 and gradually increased as Rotational speed increases, representing that it bears more toughness, since the resistance to applied load (hammer impact) at the weld joint interface is more because the quality of bonding between the two dissimilar metals was sound. Later at higher speed more than 1800rpm energy collapse drastically.

Table 10. Energy absorbed by the weld joints (No Interlayer)

Number of trails	**Friction Pressure (Mpa)**	**Friction Time(s)**	**Upset Pressure (MPA)**	**Upset Time(s)**	**Rotational Speed (RPM)**	**UTS (MPA)**	**Joules Energy (J)**
1	34.47	1.5	77.56	10	1120	0	0
2	34.47	1.5	77.56	10	1200	0	0
3	34.47	1.5	77.56	10	1300	0	0
4	34.47	1.5	77.56	10	1400	0	0
5	34.47	1.5	77.56	10	1500	142.77	17.2
6	34.47	1.5	77.56	10	1600	156.34	22
7	34.47	1.5	77.56	10	1700	234.68	28.6
8	34.47	1.5	77.56	10	1800	254.46	31.2
9	34.47	1.5	77.56	10	1900	0	0

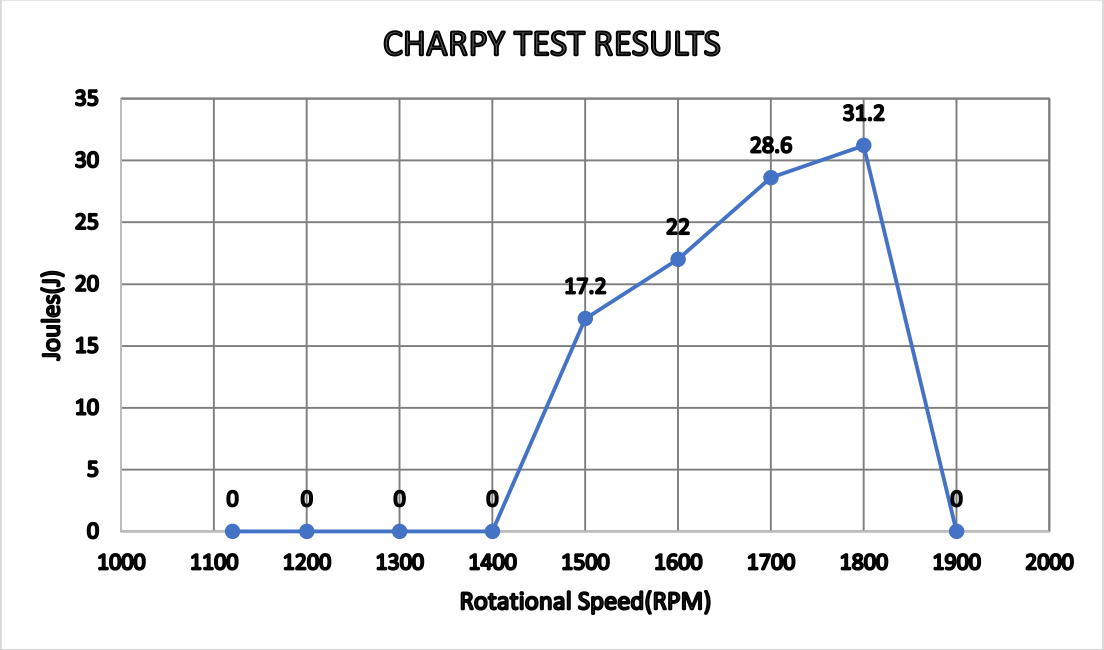

Figure 12. Joules Energy (No Interlayer)

D. Weld structure

In macrostructure level, it was observed the formation of flashes with circular symmetry, different formats, and also significant reductions in length of the cylindrical pin brass and copper in accordance with the used parameters. The below shown in fig 13 the appearance of the weld joints for 9 different trials.

Figure 13. Joints after FW

E. Evaluation of Microstructure

(EDX) analysis were conducted to investigate the phases occurring at the welding interface. These observations were made using a field-effect scanning electron microscope coupled

with EDS (energy dispersive X-ray spectroscopy) analysis. EDS point analysis was employed for the examinations. The software enabled precise control of the electron beam, allowing for surface scanning and line scanning to generate X-ray mapping and element concentration profiles, respectively.

In Figure 14, the SEM microstructure of the interface region in the friction-welded Copper-brass joint by using naval brass interlayer and the EDX analysis results are presented, illustrating the distribution of elements within the specified location. EDS analysis was performed at various points on the SEM image, as depicted in Figure 15, where EDS analysis points were defined within the interface region of the friction-welded Cu and Pb joints. The results of the EDS point analysis were correlated with the SEM findings. The EDS results provide confirmation that Cu-Pb joints contain certain intermetallic compounds. Consequently, the formation of brittle intermetallic compounds contributes to the weakening of the joint's strength

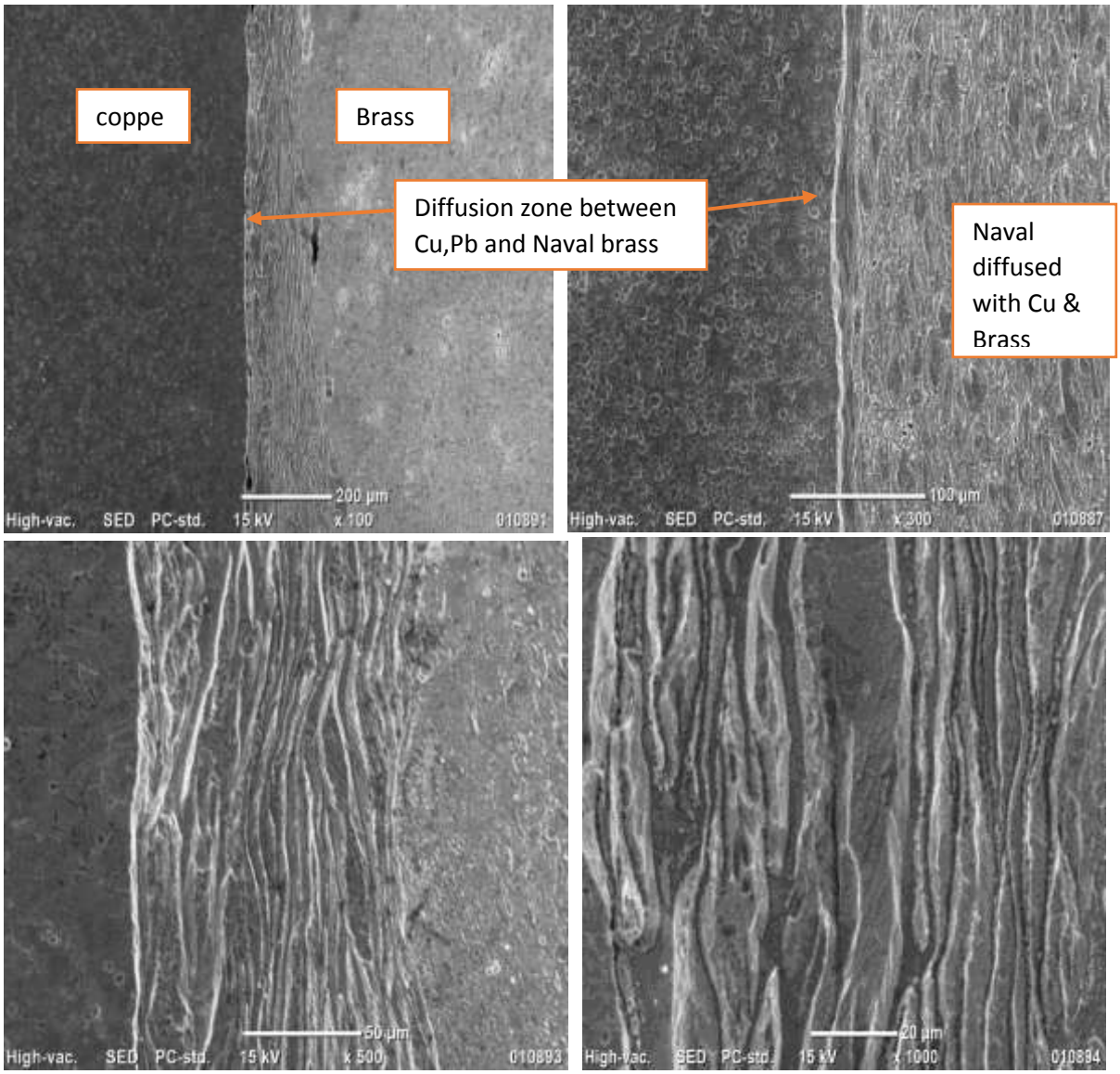

Figure 14. Microstructure images indicating diffusion zone after weld

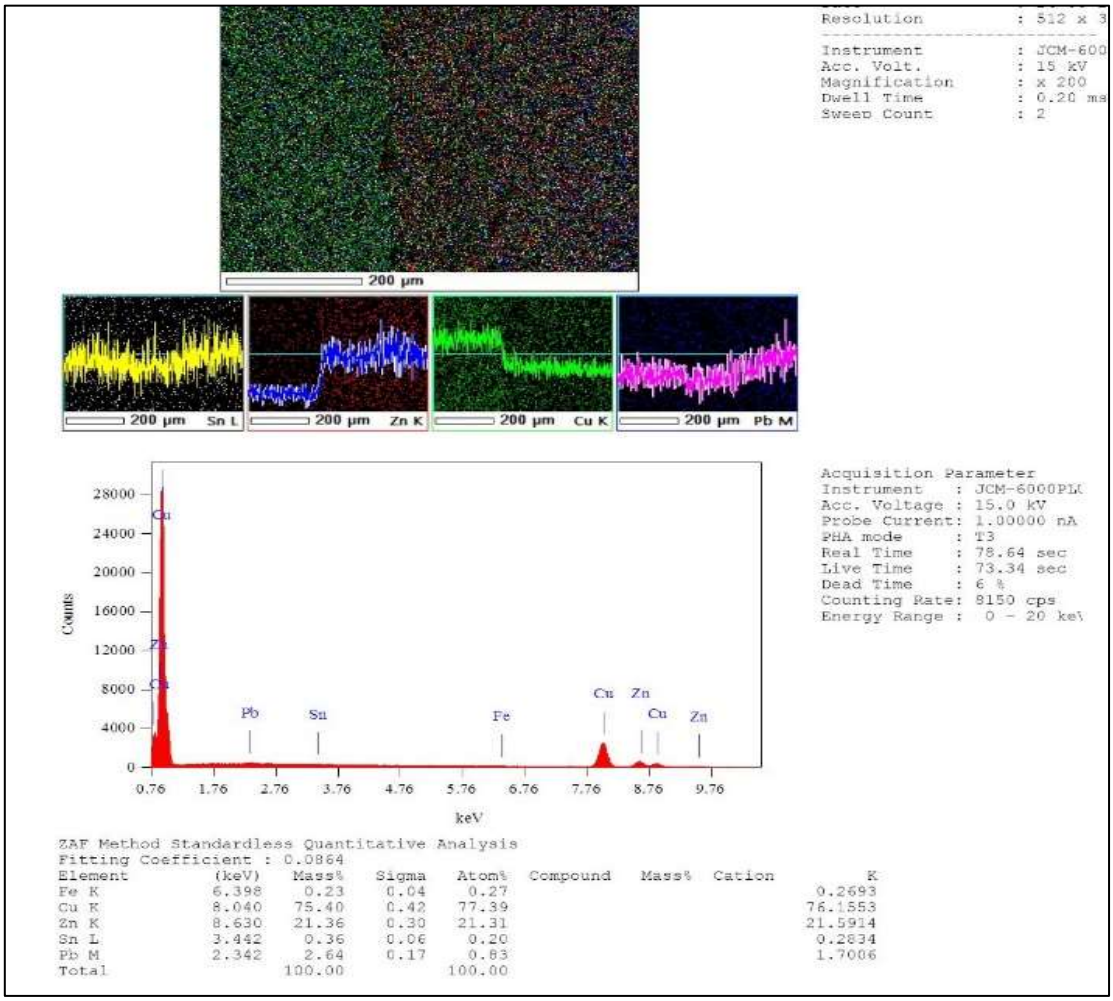

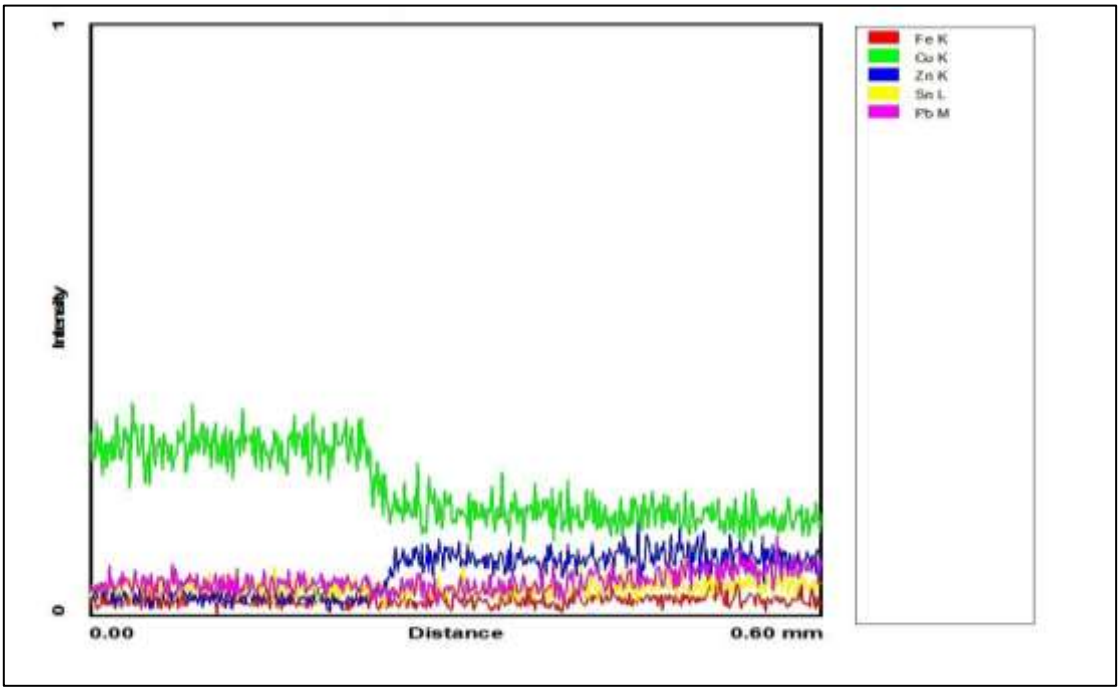

Figure 15. SEM and EDS line scanning Results of Copper and Brass with inter layer of Naval brass

In Figure 16, the SEM microstructure of the interface region in the friction-welded Copper-brass joint and the EDX analysis results are presented, illustrating the distribution of elements within the specified location. EDS analysis was performed at various points on the SEM image, as depicted in Figure 17, where EDS analysis points were defined within the interface region of the friction-welded Cu and Pb joints. The results of the EDS point analysis were correlated with the SEM findings. The EDS results provide confirmation that Cu-Pb joints contain certain intermetallic compounds. Consequently, the formation of brittle intermetallic compounds contributes to the weakening of the joint's strength

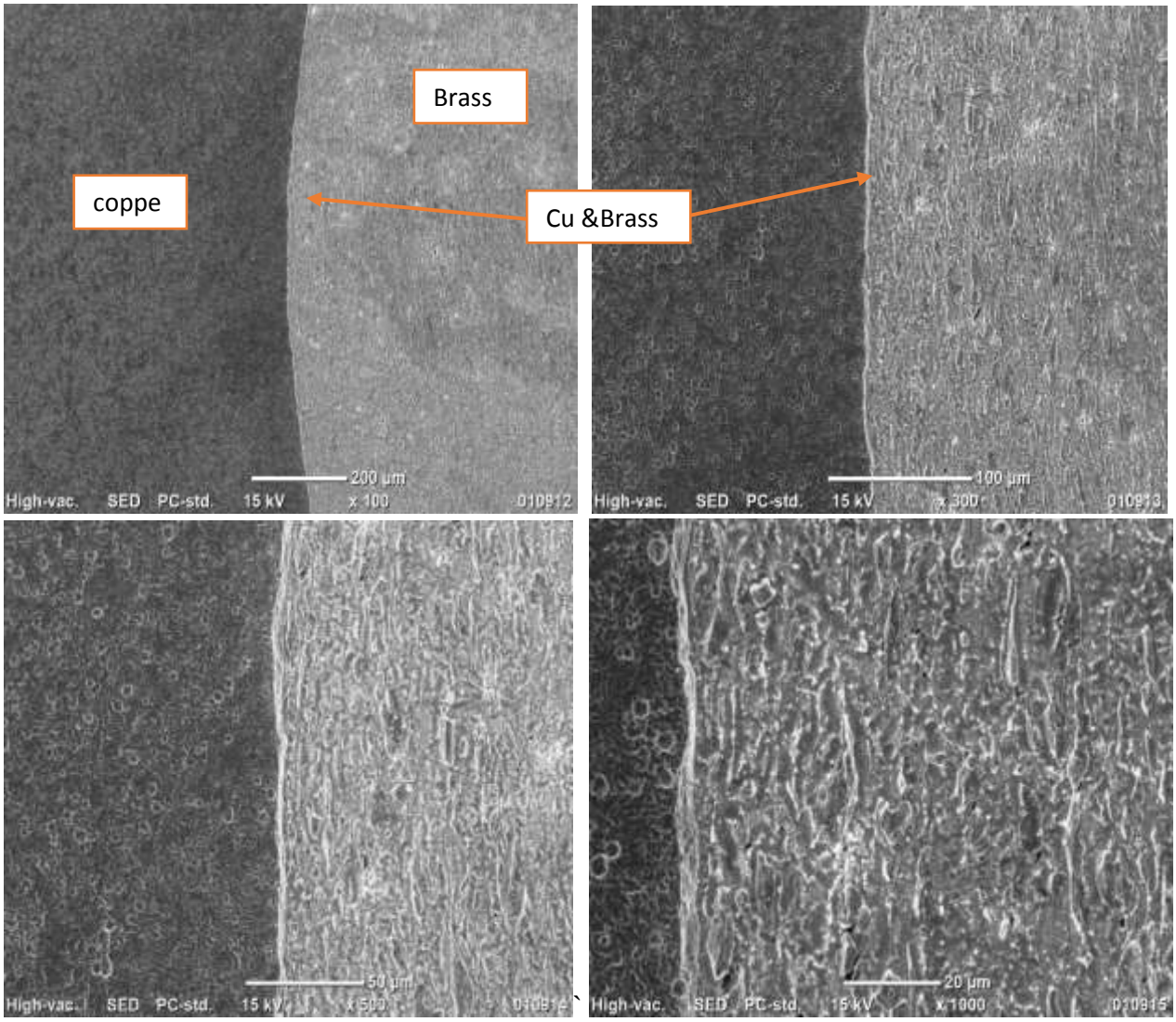

Figure 16. Microstructure images indicating diffusion zone after weld

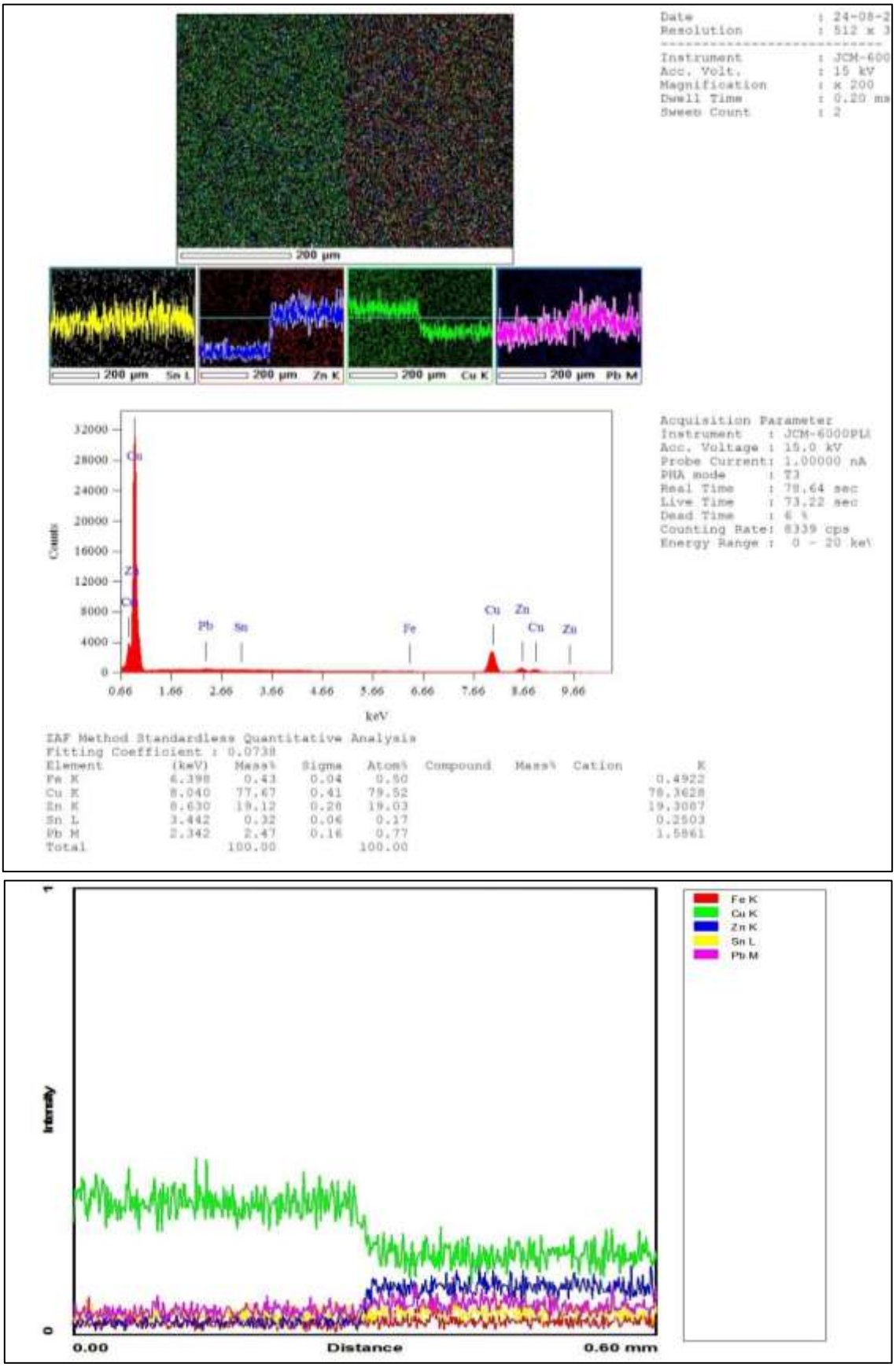

Figure 17. SEM and EDS line scanning Results of Copper and Brass

5. Conclusions:

This study delves into the application of continuous friction welding on copper and brass materials, both with and without the inclusion of a naval brass interlayer.

Different naval brass thicknesses were employed, resulting in a range of distinct outcomes outlined below:

- The tensile stress exhibited an increase as the naval brass thickness was raised from 1mm to 1.4mm but sharply declined when the thickness was further increased to 1.6mm. This phenomenon may be attributed to inadequate material flow between the metal components, leading to an insufficient intermetallic bond.
- Following the ultimate tensile strength (UTS), there was a notable alteration in the impact test results, initially showing an increase and then experiencing a significant drop as the naval brass thickness was increased.

Various frictional speeds were employed in the absence of naval brass, resulting in a spectrum of distinct outcomes detailed below:

- Initially, at 1120 rpm, no weld was achieved due to the presence of an intermetallic bond between the base metals of copper and brass. Bonding began to occur at higher speeds, specifically at 1500 rpm, 1600 rpm, and 1700 rpm.
- At 1800 rpm, a successfully welded joint was formed under the following conditions: a friction pressure of 34.47 MPa, a friction time of 1.5 s, a forge pressure of 77.56 MPa, and a forge time of 10 s. This joint demonstrated 100% joint efficiency, with the brass base metal fracturing without any cracking at the weld interface. Furthermore, the as-welded joint displayed no presence of intermetallic compound layers at the weld interface, as confirmed through SEM observations

There is still untapped potential for improving the mechanical properties of the weld interface between brass and copper by exploring adjustments to various friction parameters beyond just altering the friction speed.

References

[1] Sassani, F., & Neelam, J. R. (1988). Friction Welding of Incompatible Material.

[2] Kimura, M., Suzuki, K., Kusaka, M., Kaizu, K. (2017). Effect of friction welding condition on joining phenomena, tensile strength, and bend ductility of friction welded joint between pure aluminum and AISI 304 stainless steel.

[3] Liang, Z., Qin, G., Geng, P., Yang, F., Meng, X. (2017). Continuous drive friction welding of 5A33 Al alloy to AZ31B Mg alloy.

[4] Rajan, S. P., Kumaran, S. S., Kumaraswamidhas, L. A. (2016). An investigation on SA 213 tube to SA 387 tube plate with backing block arrangement in friction welding process.

[5] Firmanto, H. (2023). Tensile Strength and Microstructure of Rotary Friction-Welded Carbon Steel and Stainless-Steel Joints.

[6] Meshram, S. D., Reddy, G. M. (2015). Friction welding of AA6061 to AISI 4340 using silver interlayer.

[7] Rafi, H. K., Ram, G. D. J., Phanikumar, G., Rao, K. P. (2010). Microstructure and tensile properties of friction welded aluminum alloy AA7075-T6.

[8] Moinuddin, S. Q., Cheepu, M. (2023). Analysis on Bonding Interface during Solid State Additive Manufacturing between 18Cr-8Ni and 42CrMo4 High Performance Alloys.

[9] Stütz, M., Pixner, F., Wagner, J., Reheis, N., Raiser, E., Kestler, H., Enzinger, N. (2018). Rotary friction welding of molybdenum components.

[10] Sathiyaa, P., Aravindan, S., Haq, A. N., Paneerselvam, K. (2018). Optimization of friction welding parameters using evolutionary computational techniques.

[11] Bisadi, H. A., Tavakoli, A., Sangsaraki, M. T. (2013). The influences of rotational and welding speeds on microstructures and mechanical properties of friction stir welded Al5083 and commercially pure copper sheets lap joints.

[12] Reddy, G. M., Ramana, P. V. (2012). Role of nickel as an interlayer in dissimilar metal friction welding of maraging steel to low alloy steel.

[13] Yohanes, Y., Abdurrahman, R., Ridwan, A. (2019). Finite element study on rotary friction welding process for mild steel.

[14] Muralimohan, C. H., Muthupandi, V., Sivaprasad, K. (2014). Properties of Friction Welding Titanium-stainless Steel Joints with a Nickel Interlayer.

[15] Vyas, H. D., Mehta, K. P., Badheka, V., Doshi, B. (2021). Friction welding of dissimilar joints copper-stainless steel pipe consist of 0.06 wall thickness to pipe diameter ratio.